ON THE INTERACTION OF ULTRASOUND WITH CRACKS:

APPLICATIONS TO FATIGUE CRACK GROWTH

O. Buck, R.B. Thompson, and D.K. Rehbein
Iowa State University
Ames, Iowa 50011

Partial contact of two rough fatigue crack surfaces leads to transmission and diffraction of an acoustic signal at those contacts. This paper deals with recent experimental and theoretical efforts to understand and quantify such contact in greater detail. The final objective is two-fold: 1. To develop an understanding of the closure phenomenon and its application to the interpretation of fatigue data, in particular the R-ratio, spike overload/underload and threshold effects on crack propagation. 2. To obtain an understanding of the effects of closure on the detection probability of fatigue cracks, which reflects strongly on the capability for accurate life prediction. In the present paper only the first objective will be discussed.

INTRODUCTION

It has been pointed out (ref. 1) that the ultrasonic interrogation of components for the detection and sizing of defects has advantages over other techniques in that both surface as well as subsurface defects can be probed. However, it has become clear that this is not a simple problem since the phenomenon of crack closure or crack surface contact can contribute to the transmission of ultrasound across the crack surfaces which reduces the detectability and leads to erroneous crack sizing (ref. 2). Originally, the term "crack closure" was used to describe the observation of a nonlinearity in the crack opening displacement as a specimen, containing a crack, is cyclically loaded (ref. 3). It has been demonstrated that this is mainly a result of individual contact points (asperities) caused by a mismatch of the fracture surfaces (ref. 4). As this contact occurs, the stresses ahead of the crack will be redistributed such that the driving force for crack propagation becomes significantly smaller than would be expected from a simple calculation of the stress intensity range $\Delta K = K_{max} - K_{min}$ (refs. 2,3). Therefore, crack closure will affect crack propagation rates (refs. 3, 5, 6) in addition to the acoustic effects mentioned above.

*This work was supported by USDOE, Office of Basic Energy Sciences, Division of Materials Sciences under contract No. W-7405-Eng-82.

Using ultrasonic techniques, the characterization of the size and spatial variation of the local contacts, as well as the local contact stresses, is now in progress (refs. 7-15). As soon as these quantities have been fully determined it will be possible to calculate the residual stresses along the fracture surface (refs. 16, 17) which have to be overcome by the external forces in order to open the crack fully. This residual stress field is compressive and will have to be continuous with that of the plastic zone due to reverse yielding (ref. 18). Eventually it will yield full information on the "effective" stress intensity range (ref. 19), as indicated in this paper.

The purpose of the present paper is to review briefly the status of this work and to speculate on further developments which may provide valuable information on the "state" of a fatigue crack, including the "effective" stress intensity range. Only large cracks formed in non-corrosive environments will be considered here. Modifications of the closure models due to formation of corrosion debris (ref. 20) and effects of these modifications on the interaction of ultrasound with the crack have not been considered as yet.

EXPERIMENTAL TECHNIQUES

Basically two types of ultrasonic experiments have been conducted on specimens, which can be loaded in tension and compression, to study asperity contact. The first method uses the diffraction of bulk (refs. 7, 11) or surface (Rayleigh) waves (ref. 21) from locations where the contact occurs. Individual contact points can be observed in a time domain display of the signal arriving at the receiving transducer. A schematic description of a bulk wave diffraction experiment (ref. 7) is shown in Figure 1. The second method uses mainly the transmission and reflection coefficient of bulk waves (refs. 8, 10, 12-15). In this case a broadband transmitter is used. The received signal is Fourier analyzed in order to obtain information on the asperity contact. In addition, mode conversion at the asperities leads to a diffraction effect which can also be studied (ref. 15). Figure 2 shows this arrangement schematically. The longitudinal transmitted signal is obtained at $\Theta = 0°$, the diffracted signals at $\Theta = 45°$.

The above experiments are special cases of a more general one in which the angle of incidence and the angle of observation may be arbitrarily chosen for all types of mode conversions. It should be pointed out here that a theory for this general case has not been developed yet. However, to provide guidance for such a theory, an experiment has been devised (see fig. 3) in which such measurements can be performed on "model" cracks with known asperity size and separation (refs. 15, 22). A (cylindrical) specimen was produced by pressing together two blocks. One of the blocks contains a photolithographically produced roughness, simulating asperity contact at the interface. Such a specimen seems to be well suited to study transmission and reflection, as well as diffraction for a wide range of angles for different roughnesses (periodic or random).

OBSERVATIONS AND INTERPRETATIONS

Making use of signals diffracted at asperities (fig. 1) seems to be the most direct way to determine the location of these asperities, at least if they are relatively large. Golan and Arone (ref. 11) recently published first results on

such an investigation using a compact tension specimen. These authors measured the signal amplitude of shear waves diffracted at each contact point as a function of applied load. Thus, knowing at which external load each individual contact opens up (determined by a loss of the diffracted signal) and assuming that the contact is elastic allowed these authors to evaluate the contact forces using a set of torque balance equations. The results indicate that the contacts do not open in a "perfect" sequence (the opening of the contacts is unrelated to the distance from the crack tip). Consequently the contact forces do not vary in a systematic way. The sizes of the contact areas have not been determined so that the individual contact stresses can not be estimated at the present time.

The usefulness of the transmission and reflection coefficient to determine asperity contact has been demonstrated by Haines (ref. 8) (based on data by Wooldridge (ref. 23)), Thompson et al. (refs. 10, 12, 13), and Rehbein et al. (ref. 15). In either case, a quasi-static model for the interaction of an ultrasonic wave with partially contacting surfaces is used. It is assumed that, when the ultrasonic wavelength is large with respect to the dimensions and separations of the contacts, their influence on an ultrasonic wave can be modeled by a pair of effective boundary conditions

$$\begin{aligned} \sigma_i + \sigma_r - \sigma_t &= 0 \quad \text{(for the stresses)} \\ u_i + u_r - u_t &= U \quad \text{(for the displacements)} \end{aligned} \tag{1}$$

where the indices i, r, and t refer to incident, reflected, and transmitted waves, respectively and U is the elastic displacement the asperities experience due to σ_t, as will be discussed below. By applying standard analysis the (frequency dependent) transmission and reflection coefficients can be calculated. Figure 4 shows, as an example, a comparison of the calculated (ref. 8) and measured (ref. 23) reflection coefficients as a function of applied stress, σ_o, obtained on steel plates with given roughness. Qualitatively good agreement has been obtained. The major difference between the Haines and Thompson approaches is in the interpretation of the quantity U. Haines (ref. 8) makes use of a detailed model of the contact between real surfaces as required to understand the physics of tribology. In this case

$$U = \frac{\sigma_t \pi \, d \, p_m}{2\sigma_o k^* E} \tag{2}$$

where d is the mean diameter of the contact area, (which can be related to surface roughness), p_m is the "flow pressure" (usually three times the ultimate tensile strength), E is the Young's modulus, σ_o is the average static stress across the interface, and k* is a constant (≈ 2). Thompson et al. (ref. 10), on the other hand, uses an analytical solution for the additional displacement which an interface experiences if this interface consists of individual contacts. For a simple strip model* one obtains

$$U = \frac{\sigma_t}{\kappa} \tag{3}$$

with

*A modification of this strip model to describe the more realistic situation of individual contact points will be discussed later.

$$\kappa = \frac{E}{2\alpha s}\left\{1.071\left(\frac{1}{\alpha}\ln\frac{1}{1-\alpha}-1\right)+0.25\alpha-0.357\alpha^2+0.121\alpha^3+\ldots\right\} \qquad (4)$$

where $\alpha = 1-w/s$, and w and s are the width and separation of the asperity contacts. Using focused, broadband acoustic transducers (see fig. 2), Thompson and Fiedler (ref. 13) determined the transmission coefficient for a fatigue crack (fig. 5a). The results can be compared with calculated values (fig. 5b) under the following assumptions. The beam profile is Gaussian and frequency dependent and the Kirchhoff approximation can be applied. κ (and therefore w and s) changes gradually from ∞ to 0 over a certain distance away from (but containing) the crack tip. A good fit to the experimental results has been obtained choosing an exponentially decaying κ. The result is that the crack length appears to be larger for the higher frequency components than for the lower ones. The independent variables w and s (Eq. 4) have not been determined separately as yet. A second type of experiment will have to be performed.

On the other hand, it should be mentioned that the frequency dependent transmission and reflection coefficients, as calculated by this model (ref. 10), have been compared to exact solutions for periodic arrays of strip contacts, as calculated by Angel and Achenbach (ref. 24). It was found that the agreement between these exact solutions and those obtained by Thompson et al. (ref. 10) is excellent when the wavelength is large with respect to the contact spacing, a condition under which most of the experiments have been performed to date. It is noteworthy, however, that the exact solutions (ref. 24) show large changes in the transmission and reflection coefficients when the wavelength is equal to the contact spacing, thus providing direct information on contact spacing.

The quasi-static model was expanded recently (refs. 15, 25) for the case of a longitudinal wave at normal incidence to the fracture surface. The model now predicts diffracted longitudinal and mode-converted transverse waves, given by the normalized signal

$$\Gamma^N = C\int_{-\infty}^{\infty} dx\left[\frac{1}{1+j\alpha}\right]e^{-(x-x_1)^2/p^2}\, e^{-jk(x-x_1)\sin\theta} \qquad (5)$$

where C is a normalizing constant involving the wave velocities, beam amplitude, beam widths and an angular term, p is a beam width parameter, k is the wave vector, x_1 is the position of the beam center and θ is the angle of the receiver with respect to the transmitter axis. For all forward transmission experiments, θ is equal to 0°; all tip diffracted experiments were performed at $\theta = 45°$ so far. The normalization is executed with respect to the through transmission signal received from the uncracked region. The bracketed factor in the equation represents the interface transmissivity and the other factors describe the beam magnitude and phase overlaps. The factor α in the bracketed term is

$$\alpha = \pi\rho v f/\kappa(x) \qquad (6)$$

where ρ is the material density, v the transmitted wave velocity, f is the frequency and $\kappa(x)$ is the distributed spring constant. Again, choosing $\kappa(x)$ to be a continuous exponential, comparison of theory and experiment at $\theta = 0°$ was favorable, as reported elsewhere (refs. 12, 13). Alternatively, the experimentally observed longitudinal and shear wave signals diffracted in the closure region of a fatigue crack, could not be predicted by the model. The more severe deviation of experiment from the model is for the shear wave case, as shown in figure 6. The frequency dependence of the signals from the real crack is much greater than those from the

ideal crack for both the model and experiment. In addition, the peak amplitude of the experimental data has decreased significantly from the corresponding peak for the ideal crack. The frequency dependence of the theoretical predictions is quite pronounced, and at the higher frequencies, the theory is several orders of magnitude too small. It would appear, therefore, that the closure region plays an even more significant role for tip diffracted shear waves than for longitudinal waves, either tip diffracted or through transmission. The model was therefore extended to (approximately) include the effects due to discrete contact points of varying diameter. In equation (5), the interface transmissivity is given by the term $1/(1+j\alpha)$. In a first attempt to assess the significance of discrete contacts, the following assumptions were made regarding the form of the dynamic crack opening displacement (COD). (1) The spatial average of the COD is the same as that predicted by the quasi-static spring model. (2) The local COD assumes the value of zero over an effective contact of diameter d and is a constant elsewhere. (3) In evaluating the ensuing scattering expressions, integrals over the small circular contact areas (with dimensions much less than a wavelength) may be approximated by the value of the integrand times the area of a circle of twice the contact diameter. When the approximate COD is substituted into the representation integral for ultrasonic scattering, the result is equivalent to that which would be obtained when the interface transmissivity is replaced by the factor

$$\frac{1}{1+j\alpha} \rightarrow \left(\frac{1}{1+j\alpha}\right)\left\{1 - \frac{j8\pi f\rho dv}{E'(1-N\pi d^2)} + \frac{1}{N^{1/2}} \sum \frac{j8\pi f\rho vd\delta(x-x_i)}{E'(1-N\pi d^2)}\right\} \qquad (7)$$

where N is the contact density (assumed to be a constant over the closed region), d is the diameter of an individual contact, $E' = E/(1-\nu^2)$ and the sum is to be evaluated over the x-coordinate of the crack.

If one views $\kappa(x)$ as being known independently, e.g. from measurements of forward transmission of longitudinal waves, then d and N are related according to

$$d(x) = 8\kappa(x)/N\pi E'. \qquad (8)$$

Thus, in this model, two parameters are needed to fully define the scattering, $\kappa(x)$ and N. The previously reported longitudinal forward transmission measurements agreed well with the continuous spring model (refs. 12, 13). Hence those measurements can be considered as an experimental determination of $\kappa(x)$. If the tip diffraction measurements are sensitive to N, they would provide an experimental means of determining this independent parameter of the partially contacting closure zone. Knowledge of both $\kappa(x)$ and N would allow the contact stresses to be calculated (refs. 12, 14).

To test this possibility, the modified model was used to calculate the 45° tip diffracted shear wave signal, as shown in figure 7. As can be seen, a change in the contact density has a marked effect on the amplitude of the peak for the 4MHz tip diffracted wave. At the lowest density considered, $N^{1/2} = 250$ contacts/cm, the theoretical predictions have increased by three orders of magnitude from the continuum limit and are approaching the level observed experimentally. In contrast, the corresponding results for longitudinal through transmission showed an indistinguishable change. It is concluded that it is essential to include discreteness of contacts in a description of tip diffracted waves and that the above scenario for directly measuring contact stress appears to hold considerable promise.

Unexpectedly large scattering effects at "model cracks", as described earlier, have been observed (refs. 15, 22). Figure 7 shows a polar plot of the signal

received for an L-wave striking an interface, with random roughness, at 45°. The comparison with the signals received from a reference block shows a surprisingly strong scattered signal in the 90° observation direction, as well as the specularly reflected signal in the 270° observation direction, obtained on the block with interface. The quasi-static model will thus have to be extended again to include the transmissivity and diffraction of crack surfaces, if the incident wave is off normal.

An interesting effect of a crack's stress history on the transmissivity was discovered using a 7075-T651 aluminum compact tension specimen. The specimen was precracked to a length of approximately 0.65 cm. At that point, the load cycling was stopped and the specimen was allowed to age for an undetermined time. The crack was then extended an additional 1 cm. The through transmission data from this specimen is shown in figure 9. In addition to the normal closure region at the tip of the crack, a second peak in the transmission coefficient data at the position of the earlier fatigue interruption can be seen. The peak becomes narrower with increasing frequency because of the smaller beam width, as at the tip of the crack. In addition, its peak value decreases at high frequencies due to the lower value of the interface transmissivity. Our current speculation is that the secondary closure peak in this data occurs in the region of the tip of the original precrack and is due to a stress overload condition that was placed on the crack when it was extended.

CONCLUSIONS

The preceeding discussions indicate that, through the use of ultrasound, it will become possible to determine the nature of asperity contact along fracture surfaces, including contact response to an external stress. Diffraction experiments (ref. 11) show that contact forces vary greatly from asperity to asperity. Transmission experiments (refs. 12-15, 25) indicate that the κ decreases with distance away from the crack tip. From Haines' model (ref. 8) and the newly developed distributed spring model (refs. 15, 25) which also uses discrete contact points, an evaluation of the contact stress present across the crack faces may now be possible through comparison of experimental data and model predictions to determine the density of asperity contacts. Once this objective is achieved, the data can be used to evaluate several characteristics of the fatigue crack, such as σ_o, the average static stress across the fracture surface (eq. 2) and, more importantly, the "effective" stress intensity range, driving the crack during propagation, as indicated below.

Combining eqs. (2) and (3) yields the average static stress to be

$$\sigma_o = \frac{\pi d p_m \kappa}{2k^* E} \tag{9}$$

and, since (ref. 8)

$$(d/2)^2 = \frac{\sigma_o}{p_m N \pi} \tag{10}$$

thus

$$\sigma_o = \left(\frac{\kappa}{k^* E}\right)^2 \left(\frac{\pi}{N}\right) p_m, \tag{11}$$

where N is the (local) number of asperities per unit area and therefore related to w and s in equation (4). The decrease in κ with distance from the crack tip suggests a similar behavior for σ_o, as one would expect for an unloaded specimen, knowing the residual stress field in front of the crack tip and the remanent crack mouth opening.

Using a simple model, Beevers et al. (ref. 18) showed that the contact of an asperity (viewed as an infinite strip) leads to a stress intensity factor K_I(local) at the crack tip for an unloaded specimen. The model is shown in figure 10a and yields

$$K_I(\text{local}) = \left(\frac{2}{\pi}\right)^{1/2} \frac{P}{BC^{1/2}} \tag{12}$$

where C is the distance from the crack tip to the asperity, B the specimen thickness and P the contact load. Using the definitions introduced earlier, the above quantities may be replaced by $C \approx s$ and $P \approx \bar{\sigma}\, Bw$ since $b \approx w$. $\bar{\sigma}$ represents the mean stress at the contact, which is related to the average static stress σ_o by, roughly, $\bar{\sigma} \approx \frac{s}{w}\sigma_o$ so that

$$K_I(\text{local}) \approx \left(\frac{2}{\pi}\right)^{1/2} \left(\frac{\kappa}{k^* E}\right)^2 \left(\frac{\pi}{N^{3/2}}\right) p_m \tag{13}$$

As an external load Q is applied, K_I(local) decreases and the compact tension specimen stress intensity factor

$$K_I(\text{global}) = \frac{f(a)Q}{B\sqrt{a}} \tag{14}$$

increases, as shown in figure 10b, where f(a) is the standard geometry factor, a the crack depth, and Q the external load. If crack closure effects are not taken into account, the driving force, ΔK, on the crack in fatigue would be

$$\Delta K = K_{Imax} - K_{Imin}. \tag{15}$$

Crack closure (ref. 3) reduces this stress intensity range ΔK to ΔK_{eff}, the "effective" stress intensity range, which can now be determined by

$$\Delta K_{eff} = K_{Imax} - K_I(\text{local}) \tag{16}$$

where K_I (local) is to be evaluated (acoustically) at the minimum load applied to the specimen and K_{Imax} is given by the geometry of the specimen, the maximum external load Q_{max} and the crack depth a by eq. (14).

The usefulness of the acoustic measurements to determine the actual crack depth a, thus providing information on K_{Imax}, and the term K_I(local) thus seems to be obvious. Its application to determine the fatigue crack propagation rate

$$da/dN = A(\Delta K_{eff})^m \tag{17}$$

as suggested originally by Elber (ref. 3), is a goal of the future. Particularly interesting will be to study cases in which the materials parameters A and m should be independent of the applied fatigue conditions, such as for stress ratio and spike overload effects.

REFERENCES

1. Silk, M. G., "Research Techniques in Non-Destructive Testing, Vol. I", ed. R. S. Sharpe, Academic Press, 1977, p. 51.

2. Buck, O., and Tittman, B. R., "Advances in Crack Length Measurement", ed. C. J. Beevers, Engineering Materials Advisory Services (EMAS), Cradley Heath, Warley, West Midlands, U. K., 1982, p. 413.

3. Elber, W., "Damage Tolerance in Aircraft Structures", ASTM STP 486, 1971, p. 230.

4. Bowles, C. Q., and Schijve J., "Fatigue Mechanisms: Advances in Quantitative Measurement of Physical Damage", ASTM STP 811, 1983, p. 400.

5. Buck, O., Frandsen, J. D., and Marcus, H. L., "Fatigue Crack Growth Under Spectrum Loads", ASTM STP 595, 1976, p. 101.

6. Suresh, S., and Ritchie, R. O., Scripta Met 17, 1983, p. 595.

7. Golan, S., Adler, L., Cook, K. V., Nanstad, R. K., and Bolland, T. K., J. Nondestructive Evaluation 1, 1980, p. 11.

8. Haines, N. F., "The Theory of Sound Transmission and Reflection at Contacting Surfaces", Report RD/B/N4711, Central Electricity Generating Board, Research Division, Berkeley Nuclear Laboratories, Berkeley, England, 1980.

9. Wooldridge, A. B., Revue du CETHEDEC 17-4, NS 80-2, 1980, p. 233.

10. Thompson, R. B., Skillings, B. J., Zachary, L. W., Schmerr, L. W., and Buck, O., "Review of Progress in Quantitative Nondestructive Evaluation, Vol 2A", eds. D. O. Thompson and D. E. Chimenti, Plenum Press, 1983, p. 325.

11. Golan, S., and Arone, R., "New Procedures in Nondestructive Testing", ed. P. Höller, Springer Verlag, 1983, p. 587.

12. Thompson, R. B., Fiedler, C. J., and Buck, O., "Nondestructive Methods for Materials Property Determination", eds. C. O. Ruud and R. E. Green, Plenum Press, 1984, p. 161.

13. Thompson, R. B., and Fiedler, C. J., "Review of Progress in Quantitative Nondestructive Evaluation, Vol. 3A", eds. D. O. Thompson and D. E. Chimenti, Plenum Press, 1984, p. 207.

14. Buck, O., and Thompson, R. B., "Fatigue 84", ed. C. J. Beevers, Engineering Materials Advisory Services, Cradley Heath, Warley, West Midlands, U. K., 1984, p. 667.

15. Rehbein, D. K., Thompson, R. B., and Buck, O., "Interaction of Ultrasonic Waves with Simulated and Real Fatigue Cracks", in "Review of Progress in Quantitative Nondestructive Evaluation, Vol. 4", eds. D. O. Thompson and D. E. Chimenti, Plenum Press (in press).

16. Westergaard, H. M., 1939, Trans. ASME (J. Appl. Mech.) 61, 1939, p. A-49.

17. Buck, O., Skillings, B. J., and Reed, L. K., "Review of Progress in Quantitative Nondestructive Evaluation, Vol. 2A", eds. D. O. Thompson and D. E. Chimenti, Plenum Press, 1983, p. 345.

18. Rice, J. R., "Fatigue Crack Propagation", ASTM STP 415, 1967, p. 247.

19. Beevers, C. J., Bell, K., Carlson, R. L., and Starke, E. A., Eng. Fract. Mechanics 19, 1984, p. 93.

20. Suresh, S., Parks, D. M., and Ritchie, R. O., "Fatigue Thresholds: Fundamentals and Engineering Applications", eds. J. Bäcklund, A. F. Blom and C. J. Beevers, Engineering Materials Advisory Services (EMAS), Cradley Heath, Warley, West Midlands, U. K., 1981, p. 391.

21. Tittmann, B. R., Ahlberg, L. A., and Buck, O., "Review of Progress in Quantitative Nondestructive Evaluation, Vol. 1", eds. D. O. Thompson and D. E. Chimenti, Plenum Press, 1982, p. 551.

22. Buck, O., Fiedler, C. J., Reed, L. K., Lakin, K. M., and Thompson, R. B., "Review of Progress in Quantitative Nondestructive Evaluation, Vol. 3A", eds. D. O. Thompson and D. E. Chimenti, Plenum Press, 1984, p. 199.

23. Wooldridge, A. B., "The Effects of Compressive Stress on the Ultrasonic Response of Steel-Steel Interfaces and of Fatigue Cracks", Report NW/SSD/RR/42/79, Central Electricity Generating Board, Northwestern Region, Manchester, England, 1979.

24. Angel, Y. C., and Achenbach, J. D., "Reflection and Transmission of Elastic Waves by an Array of Microcracks" in "Review of Progress in Quantitative Nondestructive Evaluation, Vol. 4", eds. D. O. Thompson and D. E. Chimenti, Plenum Press (in press).

25. Thompson, R. B., Fiedler, C. J., and Rehbein, D. K., Ames Laboratory, private communication.

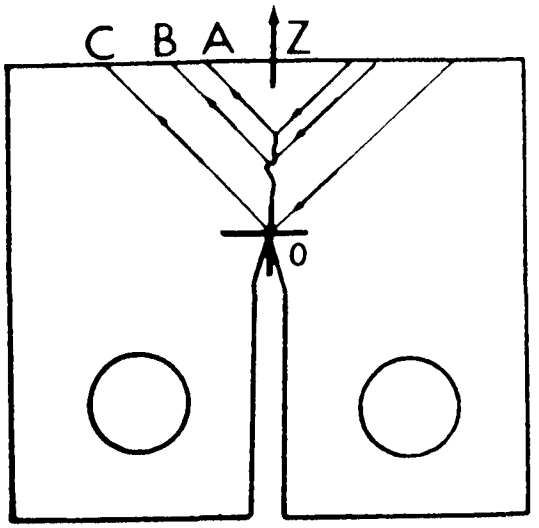

Fig. 1 Signals diffracted at contacts along the crack (ref. 7).

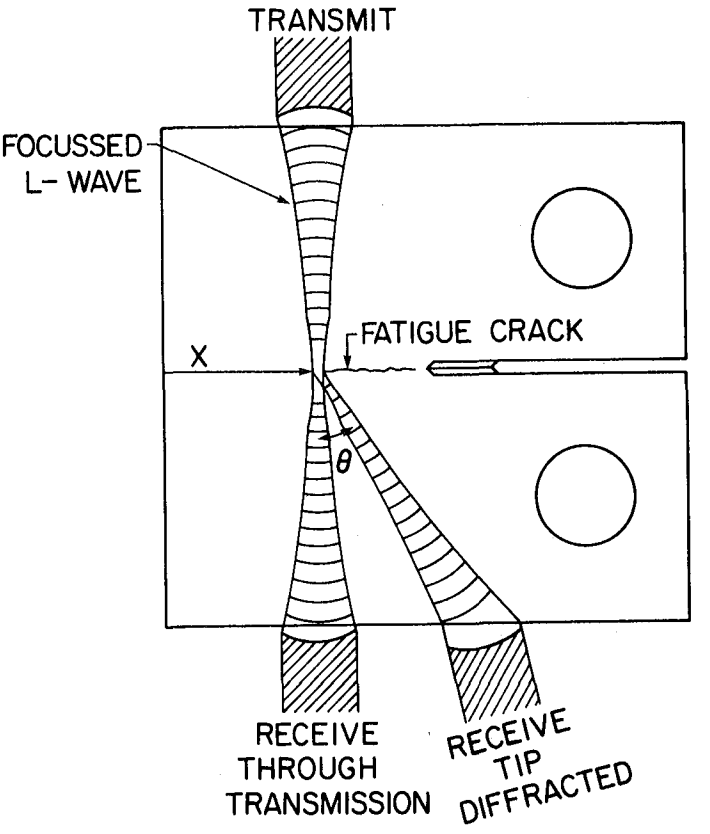

Fig. 2 Setup for obtaining crack and reference signal.

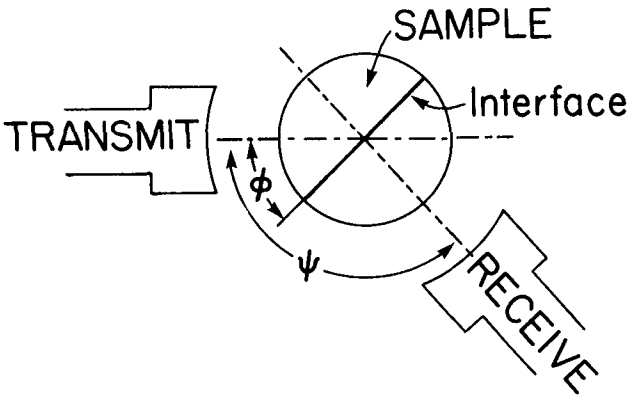

Fig. 3 Experimental setup using focussed transducers to determine scattering from interfaces in a cyclindrical sample (ref. 22).

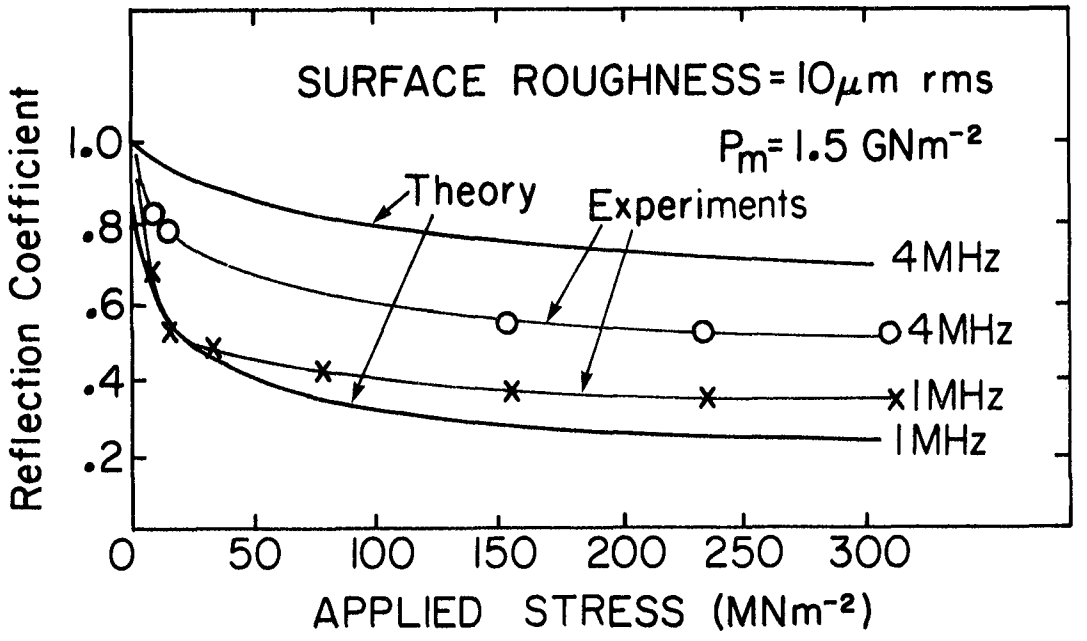

Fig. 4 Comparison of calculated and measured reflection coefficients as a function of σ_o, using shear waves (refs. 8 and 23).

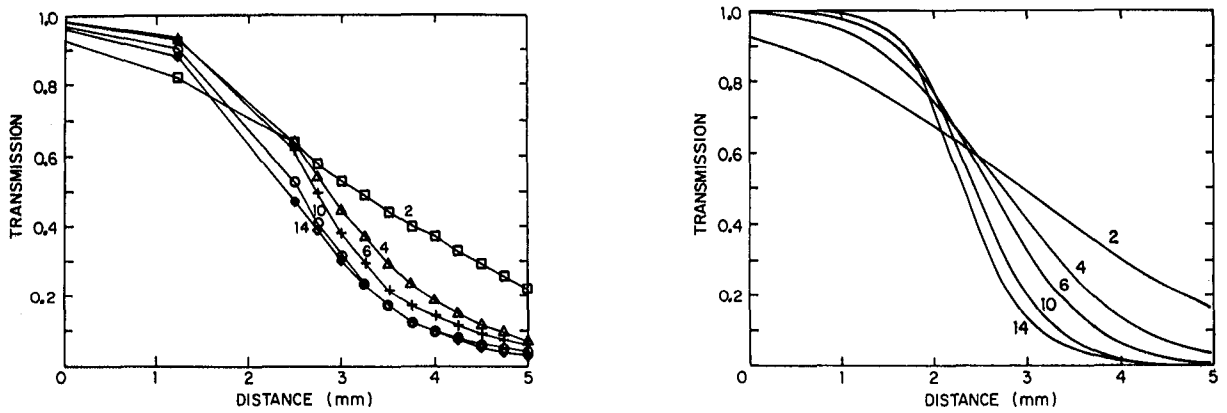

Fig. 5 Ultrasonic transmission past a fatigue crack at 2, 4, 6, 10 and 14 MHz (ref. 13). (a) experiment; (b) theory.

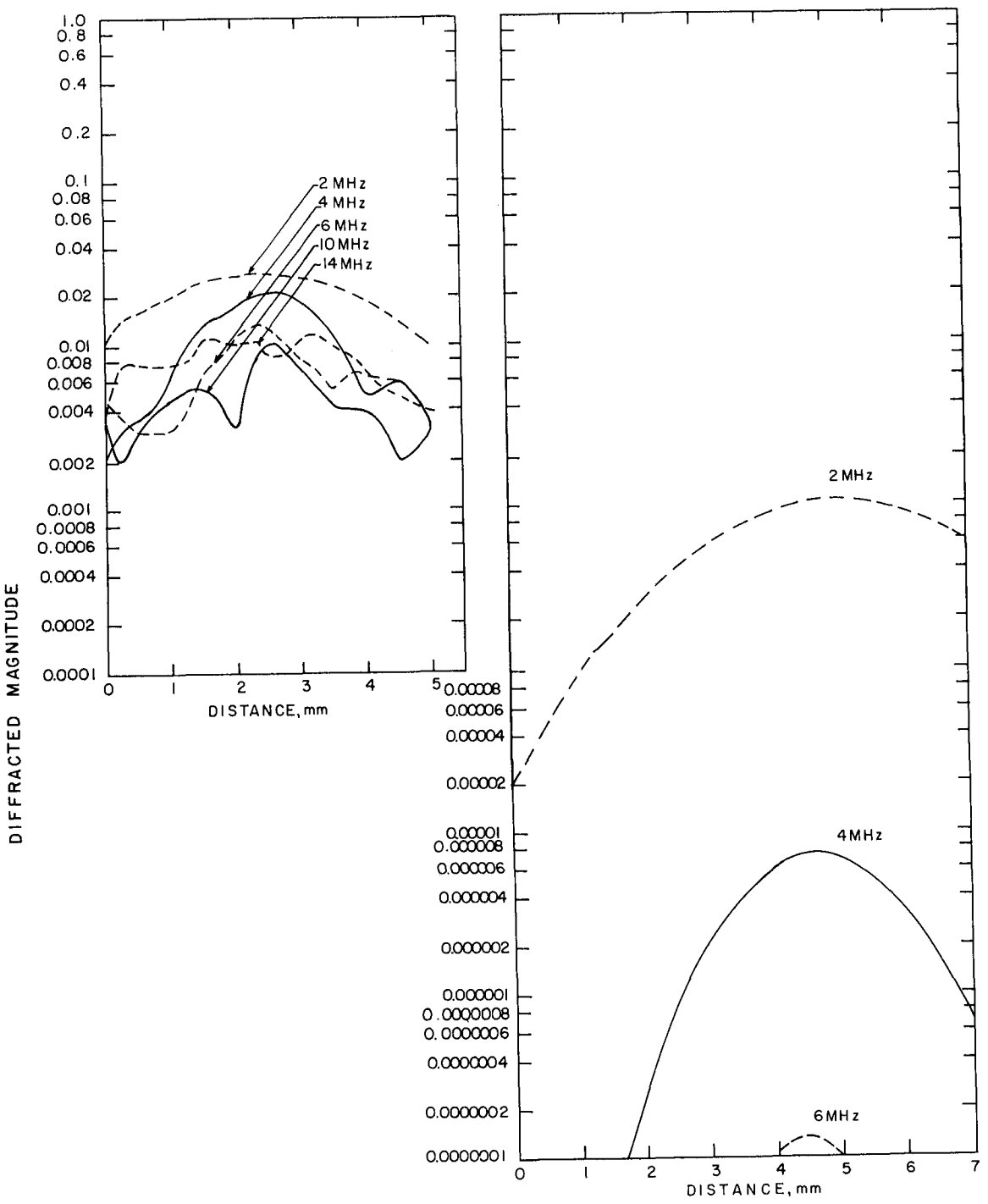

Fig. 6 Shear wave signal, mode converted in the closure region of a real crack (ref. 15). (a) experiment; (b) theory.

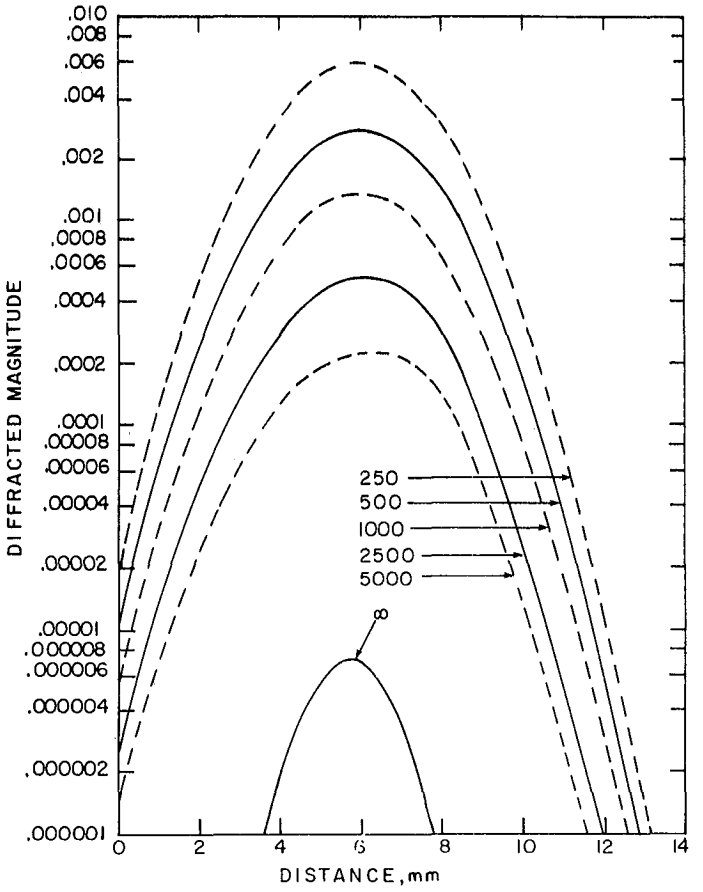

Fig. 7 Effect of contact density on the shear wave signal, mode converted in the closure region of a real crack theory (ref. 15).

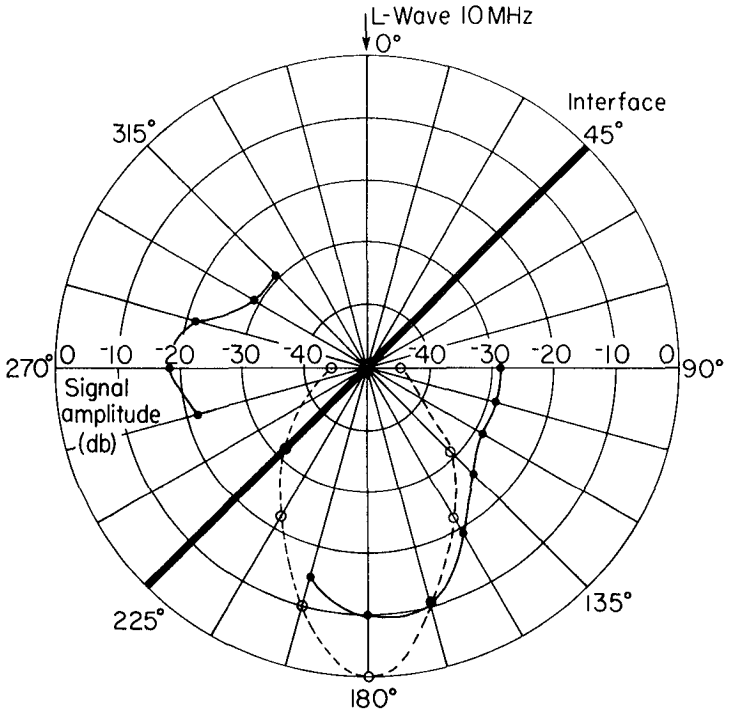

Fig. 8. Amplitudes of scattered signal (ref. 22). —— block with interface of random roughness. --- reference block (no interface).

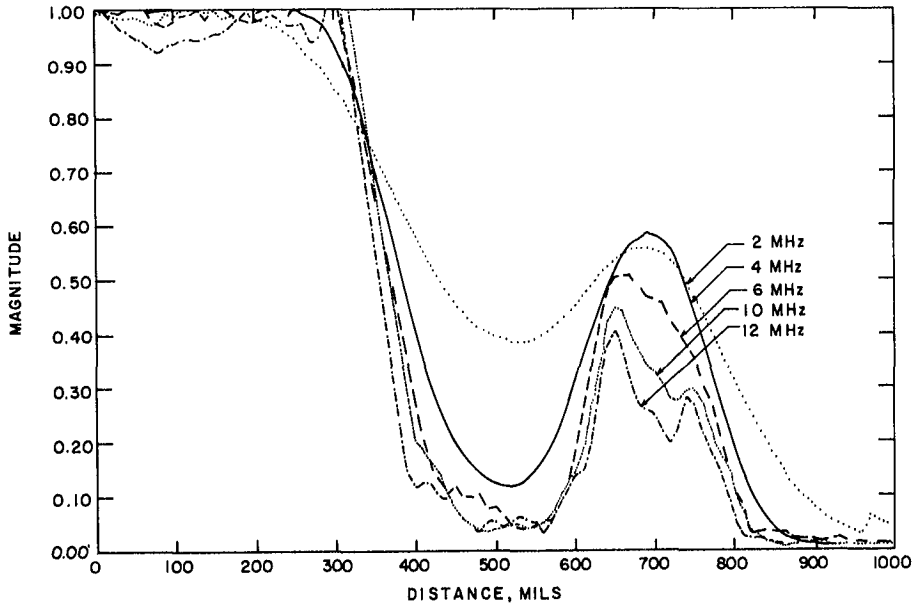

Fig. 9 Through transmission response of a fatigue crack showing partial closure far away from the crack tip (ref. 15).

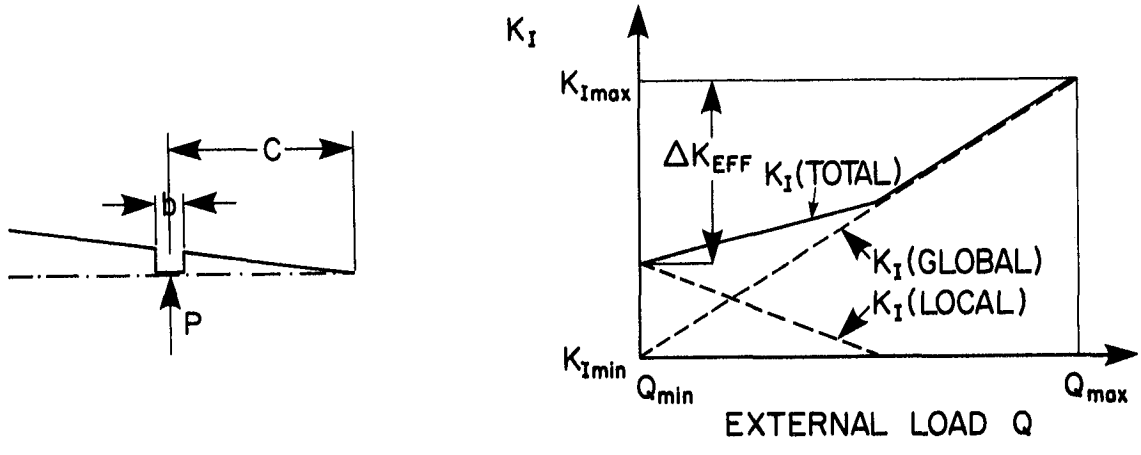

Fig. 10 (a) Model for K_I(global) and (b) Stress intensity factor as a function of external load Q.